EnMAP Technical Report

2013 Simulated EnMAP Mosaics for the Lake Tahoe region, USA

Akpona Okujeni, Sam Cooper, Karl Segl, Sebastian van der Linden, Patrick Hostert

Recommended citation of the report:

Okujeni, A., Cooper, S., Segl, K., van der Linden, S., Hostert, P., (2021), 2013 Simulated EnMAP Mosaics for the Lake Tahoe region, USA. EnMAP Technical Report, GFZ Data Services, https://doi.org/10.48440/enmap.2021.003

Supplementary datasets:

Okujeni, A., Cooper, S., Segl, K., van der Linden, S., Hostert, P., (2021), 2013 Simulated EnMAP Mosaics for the Lake Tahoe region, USA. GFZ Data Services, https://doi.org/10.5880/enmap.2021.003

Key publications:

Okujeni, A., Jänicke, C., Cooper, S., Frantz, D., Hostert, P., Clark, M., Segl, K., & van der Linden, S. (2021). Multi-season unmixing of vegetation class fractions across diverse Californian ecoregions using simulated spaceborne imaging spectroscopy data. Remote Sensing of Environment. https://doi.org/10.1016/j.rse.2021.112558

Imprint

EnMAP Consortium

Helmholtz Centre Potsdam
GFZ German Research Centre for Geosciences

Publisher
GFZ Data Services

Telegrafenberg
D-14473 Potsdam
2021

DOI: https://doi.org/10.48440/enmap.2021.003

EnMAP

Technical Report

2013 Simulated EnMAP Mosaics for the Lake Tahoe region, USA

Akpona Okujeni[1], Sam Cooper[1], Karl Segl[2], Sebastian van der Linden[3], Patrick Hostert[1]

[1] Humboldt-Universität zu Berlin, Berlin, Germany

[2] GFZ German Research Centre for Geosciences, Potsdam, Germany

[3] Universität Greifswald, Greifswald, Germany

Supported by: Federal Ministry for Economic Affairs and Energy on the basis of a decision by the German Bundestag

Table of Contents

Abstract

This dataset is composed of three-season simulated EnMAP mosaics for the Lake Tahoe region, USA. HyspIRI Airborne Campaign AVIRIS imagery from spring, summer and fall formed the basis for simulating EnMAP data with 30 m spatial resolution and 195 spectral bands ranging from 420 to 2450 nm. The mosaics are provided as Analysis-Ready-Datasets (tiled surface reflectance products) to be used for regional-scale and multi-season hyperspectral image analysis of California's diverse ecoregions. The dataset primarily intends to support the development of processing algorithms and to demonstrate spaceborne hyperspectral data capabilities during the pre-launch activities of the forthcoming EnMAP mission. This dataset was processed in line with companion simulated EnMAP mosaics for the San Francisco Bay Area (Cooper et al. 2020a) and for the Santa Barbara region (Okujeni et al. 2021a).

Coordinates:	**Centroid (Lat / Long):**	38.69° / -120.40°
	Latitude (Min / Max):	37.63° / 39.53°
	Longitude (Min / Max):	121.48° / -119.06°

Keywords: Hyperspectral Imagery, EnMAP, AVIRIS, California, Vegetation

Related sources:

An overview of the EnMAP mission is provided in Guanter et al. (2015):

Guanter, L., Kaufmann, H., Segl, K., Foerster, S., Rogaß, C., Chabrillat, S., …, and Sang, B. (2015). The EnMAP spaceborne imaging spectroscopy mission for earth observation. *Remote Sensing*, 7(7), 8830-8857. https://doi.org/10.3390/rs7070883

A full description of the EnMAP end-to-end simulation tool is described in Segl et al. (2012):

Segl, K., Guanter, L., Rogass, C., Kuester, T., Roessner, S., Kaufmann, H., Sang, B., Mogulsky, V., & Hofer, S. (2012). EeteS—The EnMAP end-to-end simulation tool. *IEEE Journal of Selected Topics in Applied Earth Observations and Remote Sensing*, 5, 522-530. https://doi.org/10.1109/JSTARS.2012.2188994

A description the across track brightness correction method is presented in Jänicke et al. (2020):

Jänicke, C., Okujeni, A., Cooper, S., Clark, M., Hostert, P., & van der Linden, S. (2020). Brightness gradient-corrected hyperspectral image mosaics for fractional vegetation cover mapping in northern California. *Remote Sensing Letters*, 11(1), 1-10. https://doi.org/10.1080/2150704X.2019.1670518

Companion studies utilizing simulated EnMAP mosaics from Californian study regions are presented in Cooper et al. (2020b) and Okujeni et al. (2021):

Cooper, S., Okujeni, A., Jänicke, C., Clark, M., & van der Linden, S., Hostert, P. (2020b). Disentangling fractional vegetation cover: regression-based unmixing of simulated spaceborne imaging spectroscopy data. Remote Sensing of Environment, 246, 111856. https://doi.org/10.1016/j.rse.2020.111856

Okujeni, A., Jänicke, C., Cooper, S., Frantz, D., Hostert, P., Clark, M., Segl, K., & van der Linden, S. (2021). Multi-season unmixing of vegetation class fractions across diverse Californian ecoregions using simulated spaceborne imaging spectroscopy data. Remote Sensing of Environment. https://doi.org/10.1016/j.rse.2021.112558

This dataset was processed in line with companion simulated EnMAP mosaics for the San Francisco Bay Area (Cooper et al. 2020a) and for the Santa Barbara region (Okujeni et al. 2021a):

Cooper, S., Okujeni, A., Jänicke, C., Segl, K., van der Linden, S., Hostert, P. (2020a): 2013 Simulated EnMAP Mosaics for the San Francisco Bay Area, USA. GFZ Data Services. https://doi.org/10.5880/enmap.2020.002

Okujeni, A., Cooper, S., Jänicke, C., Segl, K., van der Linden, S., Hostert, P. (2021a): 2013 Simulated EnMAP Mosaics for the Santa Barbara region, USA. GFZ Data Services. https://doi.org/10.5880/enmap.2021.003

1. Introduction

The Environmental Mapping and Analysis Program (EnMAP) is a German hyperspectral satellite mission that aims at monitoring and characterizing the Earth's environment on a global scale (Guanter et al., 2015). EnMAP serves to measure and model key dynamic processes of the Earth's ecosystems by extracting geochemical, biochemical and biophysical parameters, which provide information on the status and evolution of various terrestrial and aquatic ecosystems. In the frame of the EnMAP preparatory phase, pre-flight campaigns including airborne and in-situ measurements in different environments and for several application fields are being conducted. The main purpose of these campaigns is to support the development of scientific applications for EnMAP. In addition, the acquired data are input in the EnMAP end-to-end simulation tool (EeteS) and are employed to test data pre-processing and calibration-validation methods. The campaign data are made freely available to the scientific community under a Creative Commons Attribution 4.0 International License (CC BY-4.0). An overview of all available data is provided in a specifically developed metadata portal on the project website https://www.enmap.org/data_tools/flights/

This dataset is composed of three-season simulated EnMAP mosaics for the Lake Tahoe region, USA. The mosaics are provided as Analysis-Ready-Datasets (tiled surface reflectance products) to be used for regional-scale and multi-season hyperspectral image analysis of California's diverse ecoregions. The dataset primarily intends to support the development of processing algorithms and to demonstrate spaceborne hyperspectral data capabilities during the pre-launch activities of the forthcoming EnMAP mission. HyspIRI Airborne Campaign AVIRIS reflectance imagery covering the study region in multiple flight lines in spring, summer and fall 2013 was used as base data. Each AVIRIS flight line was simulated to an EnMAP-like scene with 30 m spatial resolution and 242 spectral bands ranging from 420 to 2450 nm using the EnMAP end-to-end simulator. Secondary geocorrection, across track brightness correction as well as noisy band removal were then applied to each scene. Finally, scenes were merged into simulated EnMAP mosaics, i.e., one mosaic per season, which are organized in tiles of 30 x 30 km. This dataset was processed in line with companion simulated EnMAP mosaics for the San Francisco Bay Area (Cooper et al. 2020a) and for the Santa Barbara region (Okujeni et al. 2021a).

2. Data Acquisition

HyspIRI Airborne Campaign AVIRIS imagery (Lee et al. 2015) covering the Lake Tahoe region in multiple flight lines in spring, summer and fall 2013 was used as base data for EnMAP simulation. AVIRIS imagery were downloaded from the JPL AVIRIS data portal (http://aviris.jpl.nasa.gov) as geo-corrected reflectance products with pixel resolutions between 14.4 and 16.9 m, and 224 spectral bands ranging from 370 to 2,500 nm (see Table A1 in the Appendix for an overview of individual AVIRIS flight lines). The AVIRIS pre-processing chain implemented by the Jet Propulsion Laboratory (JPL) consists of orthorectification into the UTM 10N projection (EPSG 32610), radiometric correction and atmospheric correction using a modified version of the ATmospheric REMoval program (ATREM; Thompson et al., 2015). Three acquisition dates in 2013 (Table 1) roughly correspond to different stages in plant phenological cycles. For simplicity, these three acquisitions are referred to here as spring, summer and fall.

Table 1: AVIRIS acquisition times

Campaign	Number of flight lines	Acquisition date (DD/MM/YYYY)	Acquisition time (GMT start/stop
Spring	11	02/05/2013	17:47-21:09
Summer	11	04/06/2013	17:28-20:23
Fall	11	19/09/2013	17:21-20:40

3. Data Processing and Products

Each AVIRIS reflectance image was converted into a 30 m EnMAP scene using the EnMAP end-to-end simulator (EeteS; Segl et al., 2012). In total 242 EnMAP bands were simulated from the AVIRIS imagery using the EeteS. Bands near strong atmospheric water absorption regions (1,311 – 1,465 nm and 1,783 – 2,044 nm) were removed, as were five bands in the NIR (934-952 nm) with poor reflectance retrievals. After band removal, 195 simulated EnMAP bands remained.

Across track brightness gradient correction was conducted to remove brightness gradients originating from the varying sun-sensor geometries between flight lines. A class-wise empirical across-track brightness correction approach following Schiefer et al. (2006) was implemented and describe in detail in Jänicke et al. (2020). In short, images were classified into three classes roughly corresponded to green vegetation, non-photosynthetically active vegetation (NPV) and non-vegetation. A band-wise correction factor was generated by fitting a quadratic model to each band across the range of view angles for each vegetation strata, and nadir normalized values were created by dividing the reflectance of a given pixel by the correction factor derived from the pixel's class and across-track location. The non-vegetation class, corresponding to water and urban areas were corrected with the NPV class.

While initial orthorectification was carried out by JPL, georeferencing errors were still observed in the imagery. A secondary geometric correction was therefore applied to each flight line by co-registering the simulated EnMAP flight lines to contemporaneous Landsat imagery. Tie points were automatically generated using the Automated and Robust Open-Source Image Co-Registration Software (AROSICS; Scheffler et al., 2017). Estimated local shifts ranged from less than 3 m to greater than 150 m. The EnMAP imagery was corrected using these tie points with a third-degree polynomial and bilinear resampling, and remaining residual shifts were observed only at subpixel levels.

The corrected images were then mosaicked into a single image, with western flight lines overlaying eastern flight lines. The final data configuration of the EnMAP simulations are described in Table 2.

Table 2: Simulated EnMAP data description

Simulated EnMAP Data Description	
Units	Surface Reflectance (*10,000)
Geometric Resolution	30 m x 30 m
Spectral Bands	195
Spectral Range	423 – 2439 nm
Spectral Sampling Distance	6.5 nm (VNIR), 10 nm (SWIR)
Projection	UTM 10N EPSG: 32610

4. File Description

4.1. File Format

Band Sequential Image File [*.bsq] and file header [*.hdr]

4.2. Data Content and Structure

To facilitate data storage and access, the simulated EnMAP mosaics have been organized into regular, non-overlapping tiles of 30 x 30 km (Figure 1):

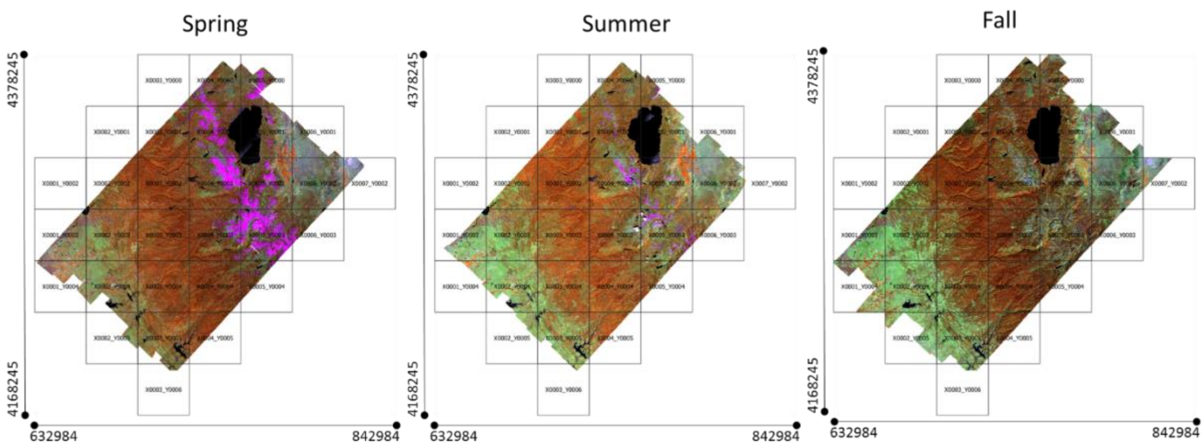

Figure 1: Spring, summer and fall simulated EnMap mosaics for the Lake Tahoe region. The underlying tiling system is indicated by the black boxes.

The data structure of the simulated EnMAP mosaic is illustrated in Figure 2. Each tile is named by its position in an x/y grid scheme originating in the north west corner of the imagery, and a shapefile is provided containing the tile locations and names.

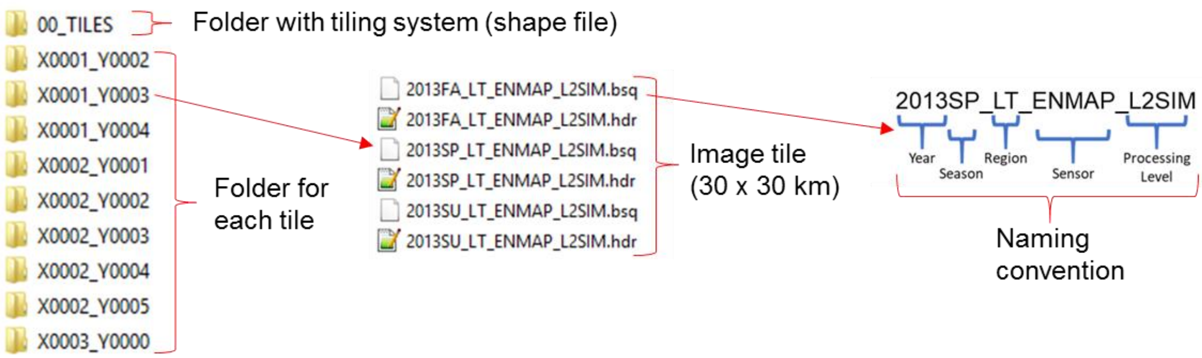

Figure 2: Data structure of the spring, summer and fall simulated EnMap mosaics for the Lake Tahoe region.

All image files from a given EnMAP scene and tile share a common naming convention: Year (2013) and Season (SP: Spring, SU: Summer, FA: Fall) indicate the acquisition timeframe. Region (LT: Lake Tahoe), indicates the region in the context of the HyspIRI Preparatory Flight Campaign. The processing level represents the in-house processing stage, were L2 indicates it is a reflectance image with secondary geometric and brightness corrections applied to the imagery and SIM indicates it is a simulated dataset of the listed sensor.

Image files are described in the header file by the following attributes: ENVI description, samples, lines, bands, header offset, file type, data type, interleave, byte order, map info, coordinate system string, wavelength units, band names, wavelength, full width half maximum (fwhm).

5. Dataset Contact

Akpona Okujeni
Email: akpona.okujeni@geo.hu-berlin.de

Sam Cooper
Email: sam.cooper@geo.hu-berlin.de

Sebastian van der Linden
Email: sebastian.linden@uni-greifswald.de

6. Acknowledgements

We would like to thank NASA Jet Propulsion Laboratory (JPL) for providing AVIRIS imagery. The simulated EnMAP mosaic was generated as part of the EnMAP Core Science Team activities funded by the German Aerospace Centre (DLR) Space Administration and granted by the Ministry of Economics and Energy (BMWi; grant number 50EE1622).

7. References

Cooper, S., Okujeni, A., Jänicke, C., Segl, K., van der Linden, S., Hostert, P. (2020a): 2013 Simulated EnMAP Mosaics for the San Francisco Bay Area, USA. GFZ Data Services. https://doi.org/10.5880/enmap.2020.002

Cooper, S., Okujeni, A., Jänicke, C., Clark, M., & van der Linden, S., Hostert, P. (2020b). Disentangling fractional vegetation cover: regression-based unmixing of simulated spaceborne imaging spectroscopy data. Remote Sensing of Environment, 246, 111856. https://doi.org/10.1016/j.rse.2020.111856

Guanter, L., Kaufmann, H., Segl, K., Foerster, S., Rogaß, C., Chabrillat, S., Küster, T., Hollstein, A., Rossner, G., Chlebek, C., Straif, C., Fischer, S., Schrader, S., Storch, T., Heiden, U., Mueller, A., Bachmann, M., Mühle, H., Müller, R., Habermeyer, M., Ohndorf, A., Hill, J., Buddenbaum, H., Hostert, P., van der Linden, S., Leitão, P., Rabe, A., Doerffer, R., Krasemann, H., Xi, H., Mauser, W., Hank, T., Locherer, M., Rast, M., Staenz, K., Sang, B. (2015). The EnMAP spaceborne imaging spectroscopy mission for earth observation. *Remote Sensing*, 7(7), 8830-8857. https://doi.org/10.3390/rs70708830

Jänicke, C., Okujeni, A., Cooper, S., Clark, M., Hostert, P., & van der Linden, S. (2020). Brightness gradient corrected hyperspectral image mosaics for mapping vegetation cover fractions in the San Francisco Bay Area. *Remote Sensing Letters*. 11(1), 1-10. https://doi.org/10.1080/2150704X.2019.1670518

Lee, C.M., Cable, M.L., Hook, S.J., Green, R.O., Ustin, S.L., Mandl, D.J., & Middleton, E.M. (2015). An introduction to the NASA Hyperspectral InfraRed Imager (HyspIRI) mission and preparatory activities. *Remote Sensing of Environment*, 167, 6-19. https://doi.org/10.1016/j.rse.2015.06.012

Okujeni, A., Cooper, S., Jänicke, C., Segl, K., van der Linden, S., Hostert, P. (2021a): 2013 Simulated EnMAP Mosaics for the Santa Barbara region, USA. GFZ Data Services. https://doi.org/10.5880/enmap.2021.002

Okujeni, A., Jänicke, C., Cooper, S., Frantz, D., Hostert, P., Clark, M., Segl, K., & van der Linden, S. (under review). Multi-season unmixing of vegetation class fractions across diverse Californian ecoregions using simulated spaceborne imaging spectroscopy data. Remote Sensing of Environment. https://doi.org/10.1016/j.rse.2021.112558

Scheffler, D., Hollstein, A., Diedrich, H., Segl, K., & Hostert, P. (2017). AROSICS: An automated and robust open-source image co-registration software for multi-sensor satellite data. *Remote Sensing*, 9, 676. https://doi.org/10.3390/rs9070676

Schiefer, S., Hostert, P., & Damm, A. (2006). Correcting brightness gradients in hyperspectral data from urban areas. *Remote Sensing of Environment*, 101(1), 25-37. https://doi.org/10.1016/j.rse.2005.12.003

Segl, K., Guanter, L., Rogass, C., Kuester, T., Roessner, S., Kaufmann, H., Sang, B., Mogulsky, V., & Hofer, S. (2012). EeteS—The EnMAP end-to-end simulation tool. *IEEE Journal of Selected Topics in Applied Earth Observations and Remote Sensing*, 5, 522-530. http://doi.org/10.1109/JSTARS.2012.2188994

Thompson, D.R., Gao, B.C., Green, R.O., Roberts, D.A., Dennison, P.E., & Lundeen, S.R. (2015). Atmospheric correction for global mapping spectroscopy: ATREM advances for the HyspIRI preparatory campaign. *Remote Sensing of Environment*, 167, 64-77. https://doi.org/10.1016/j.rse.2015.02.010

8. Appendix

Table A1: Overview of AVIRIS imagery used for generating simulated EnMAP mosaics for the Lake Tahoe region. AVIRIS imagery were downloaded from the JPL AVIRIS data portal (http://aviris.jpl.nasa.gov).

Site Name	**Name**	Year	Mon-th	Day	UTC Hour	UTC Minute	Pixel Size	Solar Eleva.	Solar Azim.	Lon1	Lon2	lat1	Lat2
T13	f130502t01p00r17	2013	5	2	19	53	15.1	66.41	175.71	-121.42	-120.12	38.42	39.45
T14	f130502t01p00r18	2013	5	2	20	14	14.8	66.3	188.59	-121.33	-120.01	38.38	39.43
T15	f130502t01p00r14	2013	5	2	19	5	16.2	64.41	145.81	-121.99	-121.18	36.93	38.05
T16	f130502t01p00r19	2013	5	2	20	30	14.8	65.67	198.32	-121.16	-119.89	38.27	39.27
T17	f130502t01p00r13	2013	5	2	18	50	16.5	62.26	137.94	-122.30	-121.93	36.96	38.19
T17	f130502t01p00r16	2013	5	2	19	36	14.5	65.97	166.18	-121.19	-119.87	38.37	39.42
T18	f130502t01p00r20	2013	5	2	20	47	14.7	64.41	207.99	-120.97	-119.73	38.19	39.17
T19	f130502t01p00r12	2013	5	2	18	31	14.5	59.9	134.5	-120.89	-119.65	38.14	39.12
T20	f130502t01p00r21	2013	5	2	21	3	14.5	62.81	216.22	-120.86	-119.58	38.03	39.04
T21	f130502t01p00r11	2013	5	2	18	14	14.6	57.56	128.26	-120.76	-119.53	37.98	38.99
T22	f130502t01p00r22	2013	5	2	21	21	14.6	60.5	224.44	-120.67	-119.40	37.96	38.96
T23	f130502t01p00r10	2013	5	2	17	56	14.4	54.85	122.56	-120.61	-119.30	37.89	38.95
T13	f130604t01p00r10	2013	6	4	18	57	15.1	68.54	135.67	-121.36	-120.12	38.49	39.44
T14	f130604t01p00r11	2013	6	4	19	14	14.9	70.73	145.31	-121.27	-120.05	38.43	39.40
T15	f130604t01p00r09	2013	6	4	18	41	15	66.39	128.27	-121.18	-119.97	38.37	39.37
T16	f130604t01p00r12	2013	6	4	19	30	14.9	72.42	156.2	-121.12	-119.89	38.30	39.27
T17	f130604t01p00r08	2013	6	4	18	26	14.8	64.17	122.31	-121.00	-119.82	38.27	39.21
T18	f130604t01p00r13	2013	6	4	19	46	14.7	73.52	168.72	-120.96	-119.78	38.20	39.14
T19	f130604t01p00r07	2013	6	4	18	9	14.7	61.42	116.38	-120.90	-119.72	38.13	39.06
T20	f130604t01p00r14	2013	6	4	20	2	14.6	73.87	182.42	-120.83	-119.58	38.06	39.05
T21	f130604t01p00r06	2013	6	4	17	53	14.7	58.73	111.74	-120.73	-119.52	38.03	38.98
T22	f130604t01p00r15	2013	6	4	20	18	14.7	73.47	196.01	-120.67	-119.43	37.96	38.94
T23	f130604t01p00r05	2013	6	4	17	36	14.5	55.73	107.32	-120.59	-119.42	37.90	38.86
T13	f130919t01p00r11	2013	9	19	19	1	15.2	50.37	157.75	-121.43	-120.10	38.41	39.47
T14	f130919t01p00r12	2013	9	19	19	22	14.9	51.74	165.86	-121.67	-119.83	38.16	39.43
T15	f130919t01p00r10	2013	9	19	18	43	14.6	49.01	151.47	-121.22	-119.90	38.34	39.46
T16	f130919t01p00r13	2013	9	19	19	40	14.9	52.52	173.34	-121.31	-119.86	38.14	39.29
T17	f130919t01p00r09	2013	9	19	18	25	14.8	47.36	145.28	-121.17	-119.80	38.14	39.23
T18	f130919t01p00r14	2013	9	19	19	58	14.7	52.71	181.18	-120.99	-119.66	38.17	39.23
T19	f130919t01p00r08	2013	9	19	18	6	14.7	45.25	139.52	-120.91	-119.58	38.12	39.18
T20	f130919t01p00r15	2013	9	19	20	16	14.6	52.56	188.75	-120.90	-119.56	38.00	39.06
T21	f130919t01p00r07	2013	9	19	17	48	14.7	43.01	134.2	-120.82	-119.49	37.95	39.01
T22	f130919t01p00r16	2013	9	19	20	33	14.7	51.88	195.94	-120.69	-119.36	37.94	38.99
T23	f130919t01p00r06	2013	9	19	17	30	14.5	40.56	129.53	-120.62	-119.23	37.88	39.01